

Fusion neutron source and array of particle detectors for nondestructive interrogation of special nuclear materials

Author

Masuda, Kai, Takahashi, Yoshiyuki, Misawa, Tsuyoshi, Yamakawa, Norio, Scott, Thomas B, Bakr, Mahmoud

Published

2024

Journal Title

Journal of Applied Physics

Version

Version of Record (VoR)

DOI

[10.1063/5.0225179](https://doi.org/10.1063/5.0225179)

Rights statement

© 2024 Author(s). All article content, except where otherwise noted, is licensed under a Creative Commons Attribution-NonCommercial-NoDerivs 4.0 International (CC BY-NC-ND) license (<https://creativecommons.org/licenses/by-nc-nd/4.0/>).

Downloaded from

<https://hdl.handle.net/10072/433458>

Griffith Research Online

<https://research-repository.griffith.edu.au>

Fusion neutron source and array of particle detectors for nondestructive interrogation of special nuclear materials

Cite as: J. Appl. Phys. **136**, 114503 (2024); doi: [10.1063/5.0225179](https://doi.org/10.1063/5.0225179)

Submitted: 23 June 2024 · Accepted: 29 August 2024 ·

Published Online: 17 September 2024



Kai Masuda,¹  Yoshiyuki Takahashi,²  Tsuyoshi Misawa,²  Norio Yamakawa,³  Thomas B. Scott,⁴
and Mahmoud Bakr^{1,4,5,6,a)} 

AFFILIATIONS

¹Institute of Advanced Energy, Kyoto University, Uji, Kyoto, Japan

²Institute for Integrated Radiation and Nuclear Science, Kyoto University, Sennan-gun, Osaka, Japan

³Pony Industry Co. Ltd., Chuo-ku, Osaka, Japan

⁴School of Physics, University of Bristol, Bristol, United Kingdom

⁵on leave from the Department of Physics, Faculty of Science at Assiut University, Assiut, Egypt

⁶Astral Neutronics Ltd, Bristol, United Kingdom

^{a)}Author to whom correspondence should be addressed: mahmoud.bakrby@bristol.ac.uk

ABSTRACT

Presented herein are the outcomes of an experimental test involving a pioneering portable-active interrogation system designed for the nondestructive detection of special nuclear materials (SNMs). The system relies on the threshold energy neutron analysis concept and incorporates a portable deuterium–deuterium (DD) neutron generator producing a particle intensity of 5×10^7 n/s, coupled with three arrays of tensioned metastable fluid detectors (TMFDs) to detect secondary neutrons from the fissile material. In the presence of the fissile material, prompt fission neutrons are emitted, with an average energy of approximately 2 MeV, and around 30% of these neutrons have energies above that of the DD neutron source (2.45 MeV). The detection of a statistically significant neutron population exceeding this threshold firmly indicates the presence of SNM. TMFDs exhibit high sensitivity in efficiently detecting neutrons above the threshold while adeptly discriminating against neutrons below the threshold as well as gamma rays. This unique feature allows the interrogation system to maintain a lightweight profile without necessitating substantial shielding materials. The validation experiments involved the placement of 70 or 140 g masses of U-235 within a 1 m³ inspection volume. Measurements were carried out over 30 min intervals, repeated numerous times, both with and without U-235, at a DD neutron source intensity of 8×10^5 n/sec. Experimental count rates with natural uranium (NU) are consistently above those without NU. The probability of detection (PD) and probability of false alarm (PFA) were assessed utilizing these count rates. The DD neutron source intensity and inspection time were normalized at 5×10^7 n/sec and 90 s, respectively. The results indicated a PD of approximately 74% and 98% for detecting 70 and 140 g of U-235, respectively, with a PFA of <5%. These promising outcomes align with the specified PD (>90%) and PFA (<5%) targets outlined in ANSI standards.

© 2024 Author(s). All article content, except where otherwise noted, is licensed under a Creative Commons Attribution-NonCommercial-NoDerivs 4.0 International (CC BY-NC-ND) license (<https://creativecommons.org/licenses/by-nc-nd/4.0/>). <https://doi.org/10.1063/5.0225179>

I. INTRODUCTIONS

This work presents the results of an experimental evaluation of a groundbreaking portable-active interrogation system designed for the nondestructive detection of special nuclear materials (SNMs), particularly U-235. Detecting illicit materials used for chemical, biological, radiological, nuclear, and explosive weapons, known as

CBRNE threats, is crucial for global counter-terrorism efforts. While portable/transportable devices and stationary devices have been deployed for on-site nondestructive inspection at ports of entry, there has been a gap in addressing special nuclear materials (SNMs) such as Pu-239 and U-235.^{1–4} Global ports and seaports use passive and active detection techniques to investigate SNMs.⁵

Passive detectors are effective against radiological threats and may be utilized for detecting Pu-239. Still, they prove inadequate for U-235 due to their lower radioactivity and ease of shielding low energetic, spontaneous radiation. Existing neutron- and/or photon-based active methods for deployment in seaports and airports are often significant, and heavy shielding is required. Therefore, innovation is needed to support mobile applications that detect SNMs hidden in cargo containers, transported packages, or suspicious unattended street bags.⁶

A key challenge in neutron-based active interrogation is distinguishing secondary neutrons from neutron-induced fission reactions, indicating the presence of SNMs amidst the probing neutrons emitted by a neutron generator. To address this, our team has developed the threshold energy neutron analysis (TENA) technique,⁷ validated for detecting small amounts of U-235 in a sea freight container with a moderate neutron source intensity of 5×10^7 n/s. This requirement can be met by a portable neutron generator, making TENA potentially suitable for a fieldable portable system. To actively interrogate materials, the TENA method utilizes a continuous beam of 2.45 MeV neutrons from a deuterium–deuterium (DD) neutron generator. In the presence of fissile material, prompt fission neutrons are emitted, with approximately 30% having energies higher than the maximum energy of the source neutrons. A statistically significant neutron population above this threshold strongly indicates the presence of SNM. A crucial component for a successful mobile TENA system is a fast neutron detector capable of rejecting gamma rays and neutrons with energies below the threshold without heavy shielding while efficiently detecting neutrons above the threshold.

The portable system includes a fast neutron detector named centrifugally tensioned metastable fluid detector (CTMFD), which has been validated for meeting these requirements. A preliminary examination was undertaken on U-235, yielding highly promising results. The experiments involved approximately 10 g of U-235 and utilized three CTMFDs and a neutron source producing 3×10^5 n/s DD neutrons. This prototype showcased a dependable U-235 detection capability at a 96% confidence level and established a practical foundation for a TENA-based interrogation system.⁸ The current study aims to assess the effectiveness of the proposed technique, employing the TENA method integrated with an inertial electrostatic confinement fusion (IECF) neutron source and CTMFDs as particle detectors. The goal was to interrogate 70 and 140 g of U-235 and determine the probability of detection (PD) and probability of false alarm (PFA) within the system. The paper is structured as follows: Sec. II provides a comprehensive overview of the experimental setup and conditions, detailing aspects such as the neutron source, neutron detector, and detection technique, alongside other pertinent conditions. Section III is dedicated to the presentation and discussion of the experimental results. Finally, Sec. IV summarizes the findings and proposes potential avenues for future research.

II. EXPERIMENTAL SETUP AND CONDITIONS

A. Interrogation technique

The TENA method⁷ employs a neutron-in neutron-out strategy, where a fusion-based neutron source generates probing

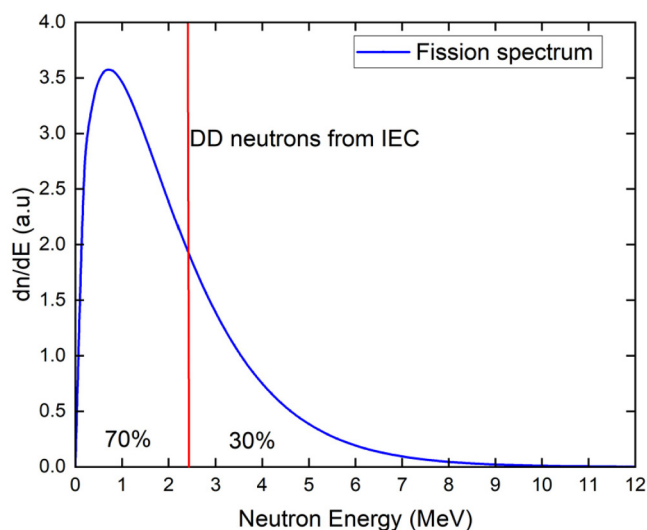


FIG. 1. The detection technique's principle is based on the TENA method, which showcases the neutron energy spectra from the SNM fission and the DD neutron source.

neutrons, and the CTMFD detects fission neutrons (secondary neutrons) emitted from the fissile material. Figure 1 depicts the fission energy spectrum of U-235 as an example. Notably, approximately 70% of the fission neutrons possess energies below that of DD neutrons, while the remaining exhibit energies above this threshold. Detecting neutrons with energies above 2.45 MeV is a distinctive signature for identifying SNMs. This distinctiveness arises because scattering tends to reduce the energies of probing neutrons, rendering the presence of neutrons above the 2.45 MeV threshold energy unique to SNMs (excluding cosmic rays). The method's validity was initially verified using DD neutrons and scintillator detectors equipped with robust gamma shielding; further details can be found in other references.⁷ Furthermore, a preliminary test was conducted to assess the technique's applicability in interrogating 10 g of U-235, yielding promising results; details can be found in Ref. 8. Other neutron sources, based on the deuterium-tritium (DT) or californium Cf252 source, are unsuitable for the detecting technique presented herein due to the overlap between the probing neutrons and the fission neutrons from the fissile material.⁹

B. Neutron source

The neutron source used in the current interrogation experiment is based on the IECF system.^{10–14} In its fundamental design, the system incorporates a negatively biased concentric grid cathode enveloped by a grounded anode utilized as a vacuum vessel. In the present configuration, a 6 cm diameter molybdenum cathode is employed, enclosed by a grounded anode featuring a 17 cm diameter Titanium inner chamber, followed by a 1 cm water jacket for anode surface cooling, with a high-voltage feedthrough junction, as depicted in Fig. 2. For further details, refer to additional sources.¹⁵

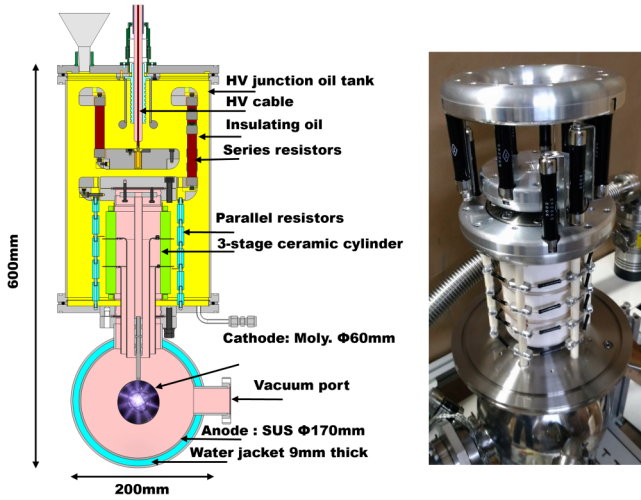
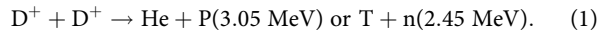


FIG. 2. A sketch of the DD neutron source (left) and the fabricated system employed in the test (right).

A potential well is formed by applying tens of kilovolts of voltage between the cathode and anode. Then, applying several tens of milliamperes current enables the ionization of fuels like D within the vacuum chamber to induce DD fusion neutron production. Initiating the discharge through tens of milliamps of current induces fusion reactions, leading to neutron and proton generation as in the following equation:



The likelihood of generating protons or neutrons is equal at 50%, but the chance of protons exiting the fusion chamber is 0% due to proton charges. IECF devices present operational advantages such as a straightforward configuration, potential for steady-state (DC) or pulsed operation modes, ease of handling, and low start-up, and maintenance costs. Consequently, they have garnered attention as neutron sources for diverse scientific research and industrial applications globally.^{16–23} The current system generated $\sim 10^8$ n/s with an input power of 5.6 kW (70 kV and 80 mA) configured in an ultracompact geometry and portable weight, with 10^9 n/s expected at a 20 kW input power. However, only 8×10^5 n/s was utilized during the current test, adhering to the facility’s radiation hazard control regulations. The distinctions between the neutron source employed in the present interrogation experiment and the one utilized in the initial test outlined in Ref. 8 are as follows: (i) the IECF system operated in a DC mode instead of a pulsed mode. (ii) The ultracompact source had a total diameter, weight, and height of 20 cm, 35 kg, and 60 cm, respectively, in contrast to 60 cm, ~ 200 kg, and 150 cm. (iii) The neutron output used in the test is 8×10^5 n/s compared to an average of 3×10^5 n/s in the previous work. Hence, the work presented herein utilizes a more minor, genuinely portable system with higher neutron output.

C. Fast neutron detector

A detector with such capability is essential to discern between the primary probing neutrons from the IECF neutron source and fission neutrons from fission processes inside the SNM. Simultaneously, the detector must be entirely immune to photons generated by the neutron source or fissile material during the interrogation. All these features are integrated into the CTMFD, lightweight, and easy to handle.²⁴ The straightforward configuration is a diamond-shaped glass pipe filled with decafluoropentane ($C_5H_2F_{10}$) as the detection liquid, connected to an adjustable-speed motor, as depicted in Fig. 3.^{25–27} The sensor’s sensitive volume is 16 cm^3 within the sensor bulb, and each rotation of the glass enclosure induces tension in the liquid, resulting in a tensioned metastable state. This tension, represented as $P_{neg}(r)$, is a function of the radial position r and can be computed using the following equation:

$$P_{neg}(r) = 2\pi^2\rho(T)\{r(T)\}^2f^2 - P_{amb}, \quad (2)$$

where ρ is the liquid density, r is the meniscus radius, f is the rotation speed, and P_{amb} is the ambient pressure.²⁸ The values of density and radius depend on the liquid temperature and strongly affect the detector’s performance. An integrated infrared sensor detects energetic neutrons triggering cavitation in the liquid. The transition from metastable liquid to stable gas occurs through localized explosive vaporization. This process selectively filters out neutrons with energies below a threshold, adjustable by modifying the rotation speed f in Eq. (2). Owing to the linear energy transfer theory, the CTMFD is impervious to photons originating from cosmic rays or generated during the interrogation process, including the discharge of the IECF device and photons from fission.²⁸ The critical distinctions between the CTMFD units employed in the current experiment and those used in the preliminary test⁸ are (i) a compact unit with approximately 50% reduction in weight, 60% reduction in size, and 80% reduction in power consumption, and (ii) the capability to operate, control, and monitor an array of units using the same software up to 50 units, in contrast to single unit control and monitoring.

CTMFD sensors (left and right arrays, each with nine units assembled in three levels) and a neutron generator are presented in Fig. 4.

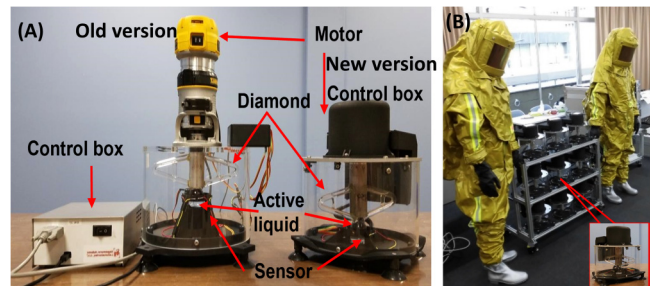


FIG. 3. Photos of the CTMFD utilized for the preliminary test (a), the lightweight unit employed in the current experiment, and the nine unit (b) array.

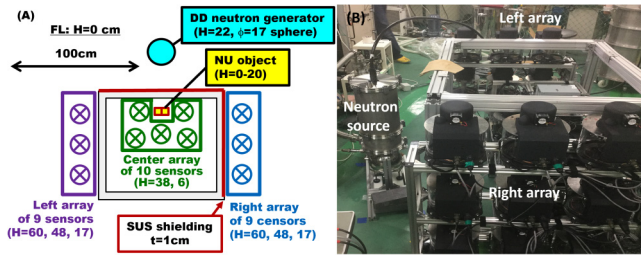


FIG. 4. Experimental layout for the interrogation of the U-235 layout (a) and a photo for the experimental setup (b).

In this layout (layout A), the front array has been relocated to the center of the inspection volume and substituted with the central array to investigate distance dependency. As shown in Fig. 4, the central array comprises ten units in two levels. The total weight of the array is less than 30 kg to facilitate the portability of the whole system. The IECF neutron source's central point is 22 cm from the floor and 40 cm from the interrogated objective. The inspection volume features 1 cm thick SS-304 plates facing the neutron generator and the right sensor array in the directions, while the left array direction remains vacant for comparison.

The test was intended to mimic a simulant positioned inside an empty cargo container, with plans to vary the inspected objective's position and content in subsequent tests. The objects targeted for detection consist of metallic natural uranium (NU) tiles stacked with polyethylene tiles, forming two objects, as illustrated in Fig. 5. These objects, labeled NU10 and NU20, weigh 10 and 20 kg, respectively, and contain approximately 71 and 142 g of U-235. Both objects are assembled to a height of 20 cm and positioned on the floor within the central array and facing the neutron source, as shown in Fig. 4.

D. Experimental conditions

Due to radiation hazard control regulations in the Kyoto University Critical Assembly (KUCA) experimental room at Kumatori Campus Osaka, the IECF neutron source was operated at 8×10^5 n/s. This operational level is two orders of magnitude less

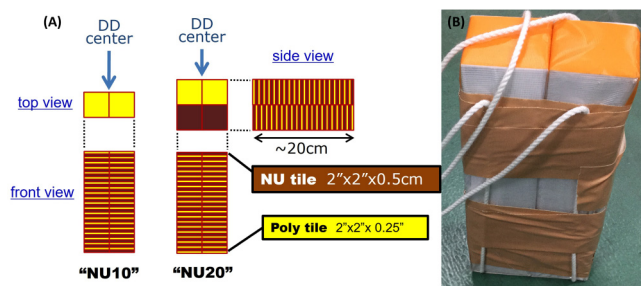


FIG. 5. (a) Top, front, and side views of the objects to be detected, NU10 and NU20; (b) photo of NU20.

TABLE I. The number of runs and run conditions.

	P_{neg} (bar)	2.4	2.8	3.2	3.6
DD 8×10^5 n/s	w/o NU	4	20	7	1
	w/NU10	...	13
	w/NU20	10	14
Cf-252, 2×10^4 or 8×10^4 n/s		3	4	3	...
BG w/o neutron source or NU		...	11

than the system's capable stable operation.^{29,30} This reduction in the neutron flux increases the interrogation time required to achieve the same detection level. The CTMFD tension, P_{neg} , was scanned at different values from 2.4 to 3.6 bar under various conditions, with and without DD neutrons, with and without NU, and with and without Cf252 at different operating schemes. There were around 90 runs, most lasting 30 min, with some runs of 15 or 60 min. After several scanning runs, P_{neg} was fixed at 2.8 bar, assuming that at this tension, CTMFDs are insensitive to neutrons with energy equal to or less than the DD neutrons (2.45 MeV), although not optimized. As previously stated, the CTMFD sensitivity to neutrons relies on the rotation speed, also called negative pressure P_{neg} as defined in Eq. (2). Most runs were conducted with NU10, NU20, and the background at $P_{neg} = 2.8$ bar; 62 runs, including 13, 14, and 20 runs, were completed with NU10, NU20, and without NU, respectively. In addition, four runs were conducted with the Cf252 source with different intensities for the detector array warming and/or calibration, and a further 11 runs without neutrons nor NU as a background. Table I shows the number of runs and the scan parameters under different conditions.

III. RESULTS AND DISCUSSION

A. Direct count rate from the CTMFD detectors

The IECF neutron source was operated at 8×10^5 n/s neutron output to interrogate NU10, NU20, and without NU. The neutron counts collected by 28 CTMFD detectors were assembled in three modules from layout A, as seen in Fig. 4. The counts from the detectors are averaged as counts per DD neutron source per detector and plotted as a function of run numbers, as illustrated in Fig. 6. It is essential to mention that only the runs with a DD source at $P_{neg} = 2.8$ bar are plotted in this figure. The error bars show a 68% confidence interval (1σ statistical error) based on the assumption of a Gaussian distribution. The figure indicates that counts from the central array with NU10 and NU20 significantly differ from those without NU from the same array. This difference can be attributed to the CTMFD sensors' high sensitivity and ability to filter out DD neutrons, which only register fission neutrons in the presence of NU.

Additionally, counts from the central array are above the counts from the left and right arrays, which can be explained by the self-shielding effect of the central units compared to those in the left and right arrays. Furthermore, the counts from the left and right arrays in the presence of NU are either slightly above or overlapped with those without NU. This observation suggests that the central units efficiently capture fission neutrons from the NU and

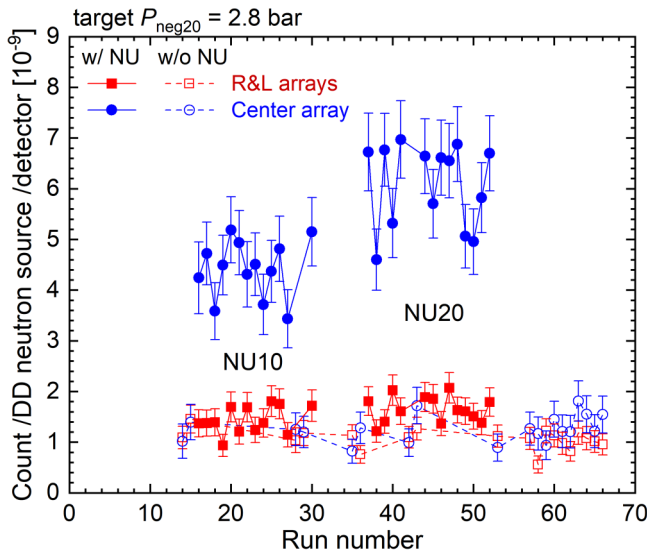


FIG. 6. Experimental count per interrogating DD neutron source per sensor on average over the CTMFD sensors in the center array and the left and right arrays, with and without the NU object in layout A.

prevent neutrons from reaching the left and right arrays. Simultaneously, the counts are consistent when the central, left, and right arrays are subjected to DD neutrons without NU.

A comprehensive analysis of the counts is performed and provided in Table II, introducing the count rate per detector (cph). The count rate per detector is defined as the accumulated count per accumulated live time over the run of the detector, with units expressed in counts per hour for each detector.

Here, \dot{n}_{BG} represents the CTMFD detectors' count rate when no neutron source nor NU is present, which could be considered the cosmic ray background. This background value will vary and depends on the location of the test. It tends to be higher in place with a nuclear research reactor in the same building, where there is the possibility of additional reactor-created residual neutrons in the experimental room.

These counts are identified as passive background counts. On the other hand, \dot{n}_{00} is the count rate with DD neutron ON and without NU presence in the runs, considered active background, which changes with the DD neutrons' intensity (\dot{n}_{00}). The ratio of passive background to active background, $\dot{n}_{BG}/\dot{n}_{00}$, on average, is

TABLE II. Analysis of the count rate per detector.

Count rate/detector (cph)	Center	Right and left
BG, \dot{n}_{BG}	1.6 ± 0.2	1.5 ± 0.1
w/o NU, \dot{n}_{00}	3.9 ± 0.2	3.3 ± 0.2
w/NU10, \dot{n}_{10}	13.2 ± 0.5	4.3 ± 0.2
w/NU20, \dot{n}_{20}	19.0 ± 0.6	5.1 ± 0.2
$\dot{n}_{BG}/\dot{n}_{00}$	0.4 ± 0.05	0.46 ± 0.05

TABLE III. The count per DD source from the interrogation.

Count/DD source (10^{-9})	Center	Right and left
w/o NU, η_{00}	0.75 ± 0.10	0.58 ± 0.07
w/NU10, η_{10}	3.91 ± 0.19	0.93 ± 0.09
w/NU20, η_{20}	5.58 ± 0.20	1.16 ± 0.08

40% at 8×10^5 n/s DD neutron intensity. While \dot{n}_{10} and \dot{n}_{20} represent the count rates when the DD neutron is ON, NU10 or NU20 are interrogated in the layout A configuration. Comparing the count rates of \dot{n}_{10} and \dot{n}_{20} , one can find a clear difference between $\dot{n}_{10}/\dot{n}_{00}$ and $\dot{n}_{20}/\dot{n}_{00}$ for the center array, showing 3.4 and 4.9 times, respectively. One can observe a clear tendency in the count rates, where $\dot{n}_{00} < \dot{n}_{10} < \dot{n}_{20}$ not only for the central array but also in the left and right arrays. This provides clear evidence of the detection of NU using the technique, as seen in Fig. 6. The observed ratio of $\dot{n}_{20}/\dot{n}_{10}$ is not double, as expected. In addition, it can be explained by considering the fission cross section's capability in the NU objects and the floor moderator effect.

Another parameter introduced in this assessment to quickly understand the performance of the detection method TENA is the count per DD neutron source (η), defined as the detection count divided by the DD neutron intensity with units of counts. When \dot{n}_{DD} changes, it leads to a change in the active background, and the relationship between them and the passive background can be expressed as $\dot{n}_{00} = \dot{n}_{BG} + \eta \dot{n}_{DD}$. Therefore, η can be given in the form $\eta = (\dot{n}_{00} - \dot{n}_{BG})/\dot{n}_{DD}$. The count rate per DD neutron source is calculated from Table II, and the results are illustrated in Table III for the runs without NU, NU10, and NU20 named η_{00} , η_{10} , and η_{20} for the central, left, and right arrays. It is evident that the values of η_{10} and η_{20} for the NU10 and NU20 surpass the value of η_{00} by 5.2 and 7.4 times for the central array, which is not the case with the left and right arrays.

Hence, the fission count per DD neutron source can be estimated from the values named $\eta_{10} - \eta_{00}$ and $\eta_{20} - \eta_{00}$ for the NU10 and NU20, respectively, and the results are presented in Table IV. Obviously, the ratio of fission per DD source for NU20/NU10 does not double with the doubling of NU for the central array, as observed and mentioned above from the count rate. In addition, statistical fluctuations make it challenging to make a definitive statement for the left and right arrays. However, the ratios of the fission count per DD neutron source for the central array to the left and right arrays were calculated and given 9.0 ± 2.9 and 8.3 ± 1.6 for NU10 and NU20, respectively. These values are consistent and agree with the geometrical ratio of the distance between

TABLE IV. The fission counts per DD source from the interrogation.

Fission count/DD source (10^{-9})	Center	Right and left
w/NU10, $\eta_{10} - \eta_{00}$	3.2 ± 0.2	0.35 ± 0.11
w/NU20, $\eta_{20} - \eta_{00}$	$4. \pm 0.2$	0.58 ± 0.11
NU20/NU10	1.5 ± 0.1	1.7 ± 0.6

the NU and the detectors in different arrays and the individual detectors' positions (horizontal and vertical) in the arrays.

B. Detection capability assessment

To assess the U-235 detection capability of the active interrogation system, adherence to a recognized standard model is crucial, such as the American National Standard Minimum Performance Criteria for Active Interrogation Systems Used for Homeland Security (ANSI standard N42.41-2021) for small articles (category A).³¹ This model envisions the interrogation of 5 kg of low-enriched uranium (LEU), incorporating approximately ~ 1 kg of U-235, within a cargo volume of $1 \times 1 \times 1$ m³. The neutron source is expected to produce 5×10^7 n/s, and the interrogation time frame is set at 90 s, with the detection system positioned outside the inspected volume. In the current experiment, the neutron intensity is 8×10^5 n/s, approximately 1/60th of the nominal interrogation intensity. Furthermore, one of the detection modules is placed inside the cargo (central array), and the interrogation time for multiple runs is set at 30 min each. Normalization of the current parameters is performed for meaningful data analysis, adjusting the neutron intensity to 5×10^7 n/s, excluding the contribution of the central array data in the assessment. The objects to be detected are NU10 and NU20, containing approximately 71 and 142 g of U-235, respectively. Figure 7 depicts various layouts for the detection capability assessment in the current experiment, encompassing the experiment, assessment, and nominal configurations based on ANSI standards.

By leveraging the experimental values of η with and without NU, the probability of detection (PD) and probability of false alarm (PFA) are computed for the neutron generator operating at an intensity of 5×10^7 n/s. This calculation is performed using the Poisson distribution function, and an alarm threshold of 23 counts per 18 sensors (N_{th}) in the left and right arrays is established within a 60 s live time (equivalent to approximately 80 s of inspection time, accounting for sensor dead time). The selection of this threshold aims to maintain PFA below 5%, aligning with ANSI standard guidelines.³¹ It is determined based on an analysis of passive and active background from the experimental results. In the Poisson distribution analysis, it is assumed that the counts from the detectors, denoted as N , follow a Poisson distribution. The mean count, N_{mean} , for the assumed Poisson distribution, is derived from N_{exp} , considering the experimental values of n_{BG} and η , along with their respective 1σ statistical errors. Two cases are contemplated: (i)

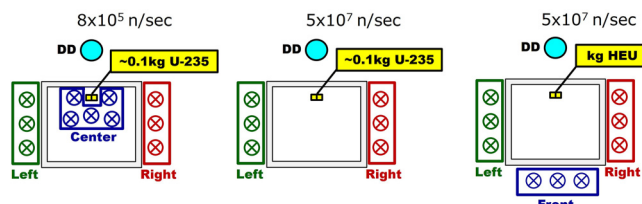


FIG. 7. Layouts for the current experiment (left) and the assessment (middle) compared to the ANSI standard (right).

TABLE V. The PD and PFA calculated from the interrogation.

Performance	Assessment		ANSI
Object to be detected	NU10	NU20	5 kg LEU
U-235 equivalent (g)	70	142	975
Inspection time (s)	90 ± 4	90 ± 3	90
PD at 68% confidence level	>74.2%	>97.8%	>90%
PFA at 68% confidence level	<3.8%	<3.6%	<5%

For counts without NU (N_{mean} w/o NU), the upper limit for a 68% probability is calculated as $N_{exp} + 0.47 \sigma(N_{exp})$. (ii) For counts with NU (N_{mean} w/NU), the lower limit for a 68% probability is calculated as $N_{exp} - 0.47 \sigma(N_{exp})$. Subsequently, the detection threshold count, N_{th} , is determined using the value from case (i) to ensure that PFA remains below 5% in adherence to ANSI standard guidelines. Furthermore, PD is calculated based on the N_{th} value derived in case (ii). The calculated values for the probability of false alarm and probability of detection, utilizing the experimental results, are summarized in Table V.

The analysis of the detection capability for NU20, as outlined in Table V, reveals a PD exceeding 97.8% and a PFA below 3.6%, indicating compliance with ANSI standard requirements. It is crucial to highlight that NU20 contains only 1/7th of the U-235 amount specified by the ANSI standard. Conversely, for NU10, the PD falls short of ANSI requirements, guiding future steps and experiments, considering 20 kg or more of NU may enhance PD and PFA acceptability. The current NU interrogation was position-specific [Fig. 7, left sketch], and future experiments will vary NU placement within the inspection volume. Filling the inspection volume (currently empty) with diverse materials aims to explore their impact on DD neutrons and/or fission neutrons. Expanding the CTMFD detector numbers to 27, organized in three arrays around the cargo container [Fig. 7, right sketch], is also planned. Precise CTMFD calibration and optimizing liquid temperature are expected to reduce passive and active background reduction. Introducing a moderator is expected to boost the fission rate and minimize active background. Upcoming plans include employing the DD source at its nominal intensity (5×10^7 n/s) to showcase PD and PFA. Exploring alternative configurations like single-sided stand-off detection and developing a larger system for scanning more extensive container categories are also on the agenda. Simulations will be conducted using Monte Carlo n-particle transport code (MCNPTC) before future experiments are planned.

IV. CONCLUSIONS

This paper presents the development of a portable-active interrogation system to detect special nuclear materials (SNMs), specifically U-235 and Pu-239. The system employs the threshold energy analysis (TENA) technique, distinguishing between probing neutrons and fission neutrons emitted from SNMs. Utilizing an inertial electrostatic confinement fusion system as a deuterium-deuterium (DD) neutron source (producing 8×10^5 n/s for the test) and tensioned metastable fluid detectors (TMFDs) for fission neutron detection, the system is designed for easy handling and

portability, weighing 35 kg for the neutron source and 27 kg of the CTMFD detector arrays. The prototype can be quickly assembled within 30 min, with an interrogation time of 2 min.

The initial evaluation involved interrogating 10 and 20 kg of natural uranium, including 70 and 142 g of U-235, placed inside a 1 m³ simulated cargo crate. Three arrays of CTMFD sensors surrounding the crate (left, right, and center) are used in the prototype. Over 90 runs were conducted, including background assessment, detector calibration, and NU interrogation. The results demonstrated promising outcomes, showing count rates from NU10 and NU20 using the central array significantly above background levels, providing straightforward evidence of successful U-235 detection using the proposed technique. Detection capability assessments were performed according to ANSI standards, normalizing neutron output to 5×10^7 n/s and interrogation time to 90 s after removing the central array's effect from the calculations. The system could detect NU20 with a probability of detection (PD) exceeding 98% and a probability of false alarm rate (PFA) below 3.6%.

Future prototypes of the active interrogation system will incorporate three modules with 27 CTMFD units surrounding the inspection object. The neutron source will operate at an intensity of 5×10^7 n/s to verify the probability of detection (PD) and probability of false alarm rate (PFA). Additionally, experiments will involve moving the object within the inspection volume to analyze the effect of the object's position on detection capability. Different cargo contents, including paper, steel, polyethylene, and aluminum, will be utilized to study the impact of material attenuation on detection. One-sided arrays will be employed, and the system will be scaled up to inspect full shipping containers, incorporating more neutron sources and detection arrays. The minimum detectable level of NU will be a key parameter in future experiments.

ACKNOWLEDGMENTS

This work was performed as a part of Projects to Support the Advancement of Strategic Core Technologies sponsored by Japan's Ministry of Economy, Trade, and Industry (METI). This work builds upon the past work supported by Special Coordination Funds for Promoting Science and Technology, sponsored by Japan's Ministry of Education, Culture, Sports, Science and Technology (MEXT). Assistance and advice from Professor Rusi Taleyarkhan and his team at Purdue University and Sagamore Adams Laboratories LLC are all highly acknowledged. One of the authors acknowledges the support of the UK's Science and Technology Facilities Council (STFC) for their partial funding assistance during the preparation of this manuscript.

AUTHOR DECLARATIONS

Conflict of Interest

The authors have no conflicts to disclose.

Author Contributions

Kai Masuda: Conceptualization (equal); Data curation (equal); Formal analysis (equal); Funding acquisition (equal); Investigation (equal); Methodology (equal); Project administration (equal);

Resources (equal); Software (equal); Supervision (equal); Validation (equal); Visualization (equal); Writing – original draft (equal); Writing – review & editing (equal). **Yoshiyuki Takahashi:** Conceptualization (supporting); Data curation (supporting); Formal analysis (supporting); Funding acquisition (supporting); Investigation (supporting); Methodology (supporting); Project administration (supporting); Resources (supporting); Software (supporting); Supervision (supporting); Validation (supporting); Visualization (supporting); Writing – original draft (supporting); Writing – review & editing (supporting). **Tsuyoshi Misawa:** Conceptualization (supporting); Data curation (supporting); Formal analysis (supporting); Funding acquisition (supporting); Investigation (supporting); Methodology (supporting); Project administration (supporting); Resources (supporting); Software (supporting); Supervision (supporting); Validation (supporting); Visualization (supporting); Writing – original draft (supporting); Writing – review & editing (supporting). **Norio Yamakawa:** Conceptualization (supporting); Data curation (supporting); Formal analysis (supporting); Funding acquisition (supporting); Investigation (supporting); Methodology (supporting); Project administration (supporting); Resources (supporting); Software (supporting); Supervision (supporting); Validation (supporting); Visualization (supporting); Writing – original draft (supporting); Writing – review & editing (supporting). **Thomas B. Scott:** Conceptualization (supporting); Data curation (supporting); Formal analysis (supporting); Funding acquisition (supporting); Investigation (supporting); Methodology (supporting); Project administration (supporting); Resources (supporting); Software (supporting); Supervision (supporting); Validation (supporting); Visualization (supporting); Writing – original draft (supporting); Writing – review & editing (supporting). **Mahmoud Bakr:** Conceptualization (lead); Data curation (lead); Formal analysis (equal); Funding acquisition (equal); Investigation (equal); Methodology (lead); Project administration (equal); Resources (equal); Software (equal); Supervision (equal); Validation (lead); Visualization (equal); Writing – original draft (lead); Writing – review & editing (lead).

DATA AVAILABILITY

The data that support the findings of the study are available from the corresponding author upon reasonable request.

REFERENCES

- ¹S. Fetter, V. A. Frolov, M. Miller, R. Mozley, O. F. Prilutsky, S. N. Rodionov, and R. Z. Sagdeev, "Detecting nuclear warheads," *Sci. Global Secur.* **1**(3–4), 225–253 (1990).
- ²A. Murata, S. Ikeda, and N. Hayashizaki, "Design of an electron-accelerator-driven compact neutron source for nondestructive assay," *Nucl. Instrum. Methods Phys. Res., B* **406**, 260–263 (2017). Available at <https://www.sciencedirect.com/science/article/pii/S0168583X16305626?via%3Dihub>.
- ³V. D. Aleksandrov *et al.*, "Application of neutron generators for high explosives, toxic agents and fissile material detection," *Appl. Radiat. Isot.* **63**(5–6), 537–543 (2005).
- ⁴M. C. Hamel, J. K. Polack, M. L. Ruch, M. J. Marath, S. D. Clarke, and S. A. Pozzi, "Active neutron and gamma-ray imaging of highly enriched uranium for treaty verification," *Sci. Rep.* **7**(1), 7997 (2017).

- ⁵J. Boo, M. D. Hammig, and M. Jeong, "Compact, lightweight imager of both gamma rays and neutrons based on a pixelated stilbene scintillator coupled to a silicon photomultiplier array," *Sci. Rep.* **11**(1), 3826 (2021).
- ⁶H. Ohgaki, I. Daito, H. Zen, T. Kii, K. Masuda, T. Misawa, R. Hajima, T. Hayakawa, T. Shizuma, M. Kando, and S. Fujimoto, "Nondestructive inspection system for special nuclear material using inertial electrostatic confinement fusion neutrons and laser Compton scattering gamma-rays," *IEEE Trans. Nucl. Sci.* **64**(7), 1635–1640 (2017).
- ⁷Y. Takahashi *et al.*, "Active neutron-based interrogation system with D-D neutron source for detection of special nuclear materials," in *Nuclear Physics and Gamma-Ray Sources for Nuclear Security and Nonproliferation* (World Scientific, 2014), pp. 341–346.
- ⁸M. Bakr, K. Masuda, Y. Takahashi, T. Misawa, N. Yamakawa, and T. Scott, "Nondestructive and active interrogation system for special nuclear material: Proof of principle and initial results," *Nucl. Sci. Tech.* **35**(1), 35:87 (1-10) (2024).
- ⁹H. Ohgaki, T. Kii, K. Masuda, M. Omer, T. Misawa, C. H. Pyeon, R. Hajima, T. Hayakawa, T. Shizuma, M. Kando, I. Daido, and H. Toyokawa, "Proposal of a nondestructive detection system for hidden nuclear materials based on a neutron/gamma-ray hybrid system," *J. Korean Phys. Soc.* **59**(5(1)), 3155–3159 (2011).
- ¹⁰R. L. Hirsch, "Inertial-electrostatic confinement of ionized fusion gases," *J. Appl. Phys.* **38**(11), 4522–4534 (1967).
- ¹¹K. Yoshikawa, K. Masuda, T. Takamatsu, S. Shiroya, T. Misawa, E. Hotta, M. Ohnishi, K. Yamauchi, H. Osawa, and Y. Takahashi, "Research and development of a compact discharge-driven D–D fusion neutron source for explosive detection," *Nucl. Instrum. Methods Phys. Res., Sect. B* **261**(1–2), 299–302 (2007).
- ¹²M. Bakr, K. Masuda, and M. Yoshida, "Improvement of the neutron production rate of IEC fusion device by the fusion reaction on the inner surface of the IEC chamber," *Fusion Sci. Technol.* **75**(6), 479–486 (2019).
- ¹³M. Bakr, T. Sakabe, J.-P. Wulfkühler, K. Mukai, T. W. Smith, Y. Ogino, M. Tajmar, T. Scott, and S. Konishi, "Influence of electrodes' geometrical properties on the neutron production rate of a discharge fusion neutron source," *Phys. Plasmas* **30**(3), 032701 (2023).
- ¹⁴S. Kenjo, Y. Ogino, K. Mukai, M. Bakr, J. Yagi, and S. Konishi, "Employing of ZrCo as a fuel source in a discharge-type fusion neutron source operated in self-sufficient mode," *Int. J. Hydrogen Energy* **47**(5), 3054–3062 (2022).
- ¹⁵R. Ahmed, G. S. Hassan, T. Scott, and M. Bakr, "Assessment of five concrete types as candidate shielding materials for a compact radiation source based on the IECF," *Materials* **16**, 2845 (2023).
- ¹⁶G. L. Kulcinski, J. F. Santarius, K. Johnson, A. Megahed, and R. L. Bonomo, "Identification of landmines and IEDs using compact fusion neutron sources on drones," *Fusion Sci. Technol.* **72**(3), 1–6 (2017).
- ¹⁷M. Bakr, R. Ahmed, T. Wallace Smith, T. Firston, and T. B. Scott, "Radiation shielding for inertial electrostatic confinement fusion system utilizing concrete and water," *J. Radiat. Res. Appl. Sci.* **17**(2), 100908 (2024).
- ¹⁸Y. Yamamoto, R. Kusaba, T. Shirouzu, and N. Inoue, "Effects of electrode shape on fusion reaction rate in a cylindrical electrostatic confinement device," *Fusion Technol.* **39**(2), 557–561 (2001).
- ¹⁹K. Takakura, T. Sako, H. Miyadera, K. Yoshioka, Y. Karino, K. Nakayama, T. Sugita, D. Uematsu, K. Okutomo, J. Hasegawa, T. Kohno, and E. Hotta, "Neutron radiography using inertial electrostatic confinement (IEC) fusion," *Plasma Fusion Res.* **13**, 2406075 (2018).
- ²⁰Y. Takahashi, T. Misawa, K. Masuda, K. Yoshikawa, T. Takamatsu, K. Yamauchi, T. Yagi, C. Ho Pyeon, and S. Shiroya, "Development of landmine detection system based on the measurement of radiation from landmines," *Appl. Radiat. Isot.* **68**(12), 2327–2334 (2010).
- ²¹K. Mukai, S. Kenjo, N. Iwamatsu, B. Mahmoud, T. Chikada, J. Yagi, and S. Konishi, "Hydrogen permeation from F82H wall of ceramic breeder pebble bed: The effect of surface corrosion," *Int. J. Hydrogen Energy* **47**(9), 6154–6163 (2022).
- ²²K. Mukai, Y. Ogino, M. I. Kobayashi, B. Mahmoud, J. Yagi, K. Ogawa, M. Isobe, and S. Konishi, "Evaluation of tritium production rate in a blanket mock-up using a compact fusion neutron source," *Nucl. Fusion* **61**(4), 046034 (2021).
- ²³M. Bakr, K. Mukai, K. Masuda, J. Yagi, and S. Konishi, "Characterization of an ultra-compact neutron source based on an IEC fusion device and its prospective applications in radiography," *Fusion Eng. Des.* **167**, 112346 (2021).
- ²⁴B. C. Archambault, J. A. Webster, J. R. Lapinskas, T. F. Grimes, and R. Taleyarkhan, "Development of a novel direction-position sensing fast neutron detector using tensioned metastable fluids," *Nucl. Instrum. Methods Phys. Res., Sect. A* **673**, 89–97 (2012).
- ²⁵T. F. Grimes, A. R. Hagen, B. C. Archambault, and R. P. Taleyarkhan, "Enhancing the performance of a tensioned metastable fluid detector based active interrogation system for the detection of SNM in 1 m^3 containers using a D–D neutron interrogation source in moderated/reflected geometries," *Nucl. Instrum. Methods Phys. Res., Sect. A* **884**(2017), 31–39 (2018).
- ²⁶B. Archambault, A. Hagen, K. Masuda, N. Yamakawa, and R. P. Taleyarkhan, "Threshold rejection mode active interrogation of SNMs using continuous beam DD neutrons with centrifugal and acoustic tensioned metastable fluid detectors," *IEEE Trans. Nucl. Sci.* **64**(7), 1781–1788 (2017).
- ²⁷J. A. Webster, A. Hagen, B. C. Archambault, N. Hume, and R. Taleyarkhan, "High-efficiency gamma-beta blind alpha spectrometry for nuclear energy applications," *J. Nucl. Eng. Radiat. Sci.* **1**(3), 031006 (2015).
- ²⁸T. F. Grimes, B. Archambault, J. A. Webster, A. Sansone, and R. P. Taleyarkhan, "Gamma-blind transformational nuclear particle sensors," in *2012 IEEE International Conference on Technologies for Homeland Security (HST)* (IEEE, 2012), pp. 417–422.
- ²⁹K. Masuda, R. Kashima, and M. A. Bakr, "Potential profile measurements inside a gridded cathode at high potential in a spherical inertial electrostatic confinement device," *Fusion Sci. Technol.* **75**(7), 608–613 (2019).
- ³⁰T. Sakabe, Y. Ogino, K. Mukai, J. Yagi, and M. Bakr, "Influence of the hydrogen isotope affinity of the cathode coating material on the neutron production rate in the glow discharge-type fusion neutron source," *Fusion Sci. Technol.* **80**(5), 653–665 (2024).
- ³¹See <https://ieeexplore.ieee.org/document/4453881> for *American National Standard Minimum Performance Criteria for Active Interrogation Systems Used for Homeland Security*, no. February (2008).